Mice lacking multidrug resistance protein 3 show altered morphine pharmacokinetics and morphine-6-glucuronide antinociception

Noam Zelcer*†‡, Koen van de Wetering*†‡, Michel Hillebrand§, Elise Sarton¶, Annemieke Kuil*, Peter R. Wielinga*, Thomas Tephly‖, Albert Dahan¶, Jos H. Beijnen§, and Piet Borst*,**

*Division of Molecular Biology and Center of Biomedical Genetics, The Netherlands Cancer Institute, Plesmanlaan 121, 1066 CX Amsterdam, The Netherlands; §Department of Pharmacy and Pharmacology, Slotervaart Hospital, 1066 EC, Amsterdam, The Netherlands; ¶Department of Anesthesiology, Leiden University Medical Center, 2333 ZA, Leiden, The Netherlands; and ‖Department of Pharmacology, University of Iowa, Iowa City, IA 52242

Contributed by Piet Borst, March 30, 2005

Glucuronidation is a major detoxification pathway for endogenous and exogenous compounds in mammals that results in the intracellular formation of polar metabolites, requiring specialized transporters to cross biological membranes. By using morphine as a model aglycone, we demonstrate that multidrug resistance protein 3 (MRP3/ABCC3), a protein present in the basolateral membrane of polarized cells, transports morphine-3-glucuronide (M3G) and morphine-6-glucuronide *in vitro*. *Mrp3*$^{(-/-)}$ mice are unable to excrete M3G from the liver into the bloodstream, the major hepatic elimination route for this drug. This results in increased levels of M3G in liver and bile, a 50-fold reduction in the plasma levels of M3G, and in a major shift in the main disposition route for morphine and M3G, predominantly via the urine in WT mice but via the feces in *Mrp3*$^{(-/-)}$ mice. The pharamacokinetics of injected morphine-glucuronides are altered as well in the absence of Mrp3, and this results in a decreased antinociceptive potency of injected morphine-6-glucuronide.

analgesia | glucuronides | morphine-3-glucuronide | transport

Morphine is a potent analgesic that acts by binding to specific opioid receptors present in the central nervous system as well as in the periphery (1, 2). A complication of morphine therapy is the development of tolerance. This necessitates an increase of dose, which changes the balance between desired and adverse side effects of morphine (1, 3). A second problem is the variability in serum concentrations of morphine and its metabolites among patients (3). The cause of this variability is probably multifactorial, including factors affecting metabolism and pharmacokinetics of morphine. Because of these problems, morphine needs to be titrated against pain intensity for each patient (1).

Of a given dose of morphine, 60–80% is excreted via the urine as glucuronidated metabolites (4, 5). The main site of morphine metabolism is the liver. In humans, morphine-3-glucuronide (M3G) and morphine-6-glucuronide (M6G) are formed in a reaction mainly catalyzed by UDP glucuronosyl transferase 2B7 (UGT2B7) (6). The pharmacological effects of M3G and M6G differ profoundly. M3G has no analgesic properties and is even thought to antagonize some of the effects of unmodified morphine (7). In contrast, M6G is more potent than morphine itself (8) and contributes to the analgesic effect of morphine (9).

Membrane transport systems have been shown to modulate the pharmacokinetics of morphine (10–13). Notably, MDR1 P-glycoprotein (P-gp), a multidrug transporter belonging to the ATP-binding cassette (ABC) family of membrane transporters and an essential component of the blood–brain barrier (13), limits morphine accumulation in the brain (10, 11). P-gp does not transport morphine-glucuronides, however (12). The increased polarity of both glucuronides relative to the parent aglycone limits their diffusion through biological membranes, and it has been suggested that specific transporters mediate their transport across the sinusoidal and canalicular membranes of hepatocytes (14, 15). ABC transporters belonging to the MRP family are known to transport organic compounds conjugated to glucuronate (16, 17). An example is MRP3 (MRP3/ABCC3), which is present in the sinusoidal membrane of hepatocytes (18–20). Substrates of MRP3 include anticancer drugs; some bile acid species; and several glucuronate, sulfate, and glutathione conjugates (20–23). MRP3 has a high affinity for glucuronidated compounds like etoposide-glucuronide and estradiol-17β-glucuronide ($E_2$17βG) (24). The fact that morphine conjugation in hepatocytes is followed by transport of the conjugate across their sinusoidal membrane, where MRP3 is located (14, 18), prompted us to study the role of MRP3 in the transport of morphine-glucuronides *in vitro*. Using *Mrp3*$^{(-/-)}$ mice (25), we have determined the pharmacokinetic and pharmacodynamic consequences of the loss of Mrp3 on morphine-glucuronide transport *in vivo*.

Materials and Methods

Materials. The hot-plate analgesia meter was from Columbus Instruments (Columbus, OH). Morphine was from the pharmacy of The Netherlands Cancer Institute. M6G was obtained from CeNeS (Cambridge, U.K.). [^{3}H]morphine (80 Ci/mmol; 1 Ci = 37 GBq and [^{3}H]$E_2$17βG 45 Ci/mmol) were purchased from Biotrend (Cologne, Germany) and PerkinElmer Life Sciences, respectively. The flow-through of solid-phase extracted urine of mice injected with [^{3}H]morphine was used as a crude [^{3}H]M3G preparation. Bondelute C18 solid-phase extraction cartridges were from Varian. Creatine phosphate and creatine kinase were from Roche Diagnostics, and RC-55L and OE-67 filters were obtained from Schleicher & Schüll. All other chemicals and reagents were from Sigma.

Cell Lines and Transient Transfections. *Spodoptera frugiperda* insect cells and HEK293 cells overproducing UGT2B7 were grown as described in refs. 24 and 6, respectively. To study the contribution of MRP3 to efflux of morphine metabolites, HEK293-UGT2B7 cells were plated in six-well plates at a density of 1×10^6 cells per well. The next day, cells were transfected by calcium phosphate precipitation with 7.5 μg of pCMVneo-MRP3 (20) or pCMVneo control. Seventy-two hours later, the medium was replaced with 3 ml of medium containing 10 μM morphine, and 250-μl samples were drawn from the medium at the indicated time points. At the

Freely available online through the PNAS open access option.

Abbreviations: ABC, ATP-binding cassette; $E_2$17βG, estradiol-17β-glucuronide; M3G, morphine-3-glucuronide; M6G, morphine-6-glucuronide; MRP, multidrug resistance protein; UGT2B7, UDP-glucuronosyltransferase 2B7; EHC, enterohepatic circulation.

†N.Z. and K.v.d.W. contributed equally to this work.

‡Present address: Howard Hughes Medical Institute, Department of Pathology and Laboratory Medicine, University of California, Los Angeles, CA 90095.

**To whom correspondence should be addressed. E-mail: p.borst@nki.nl.

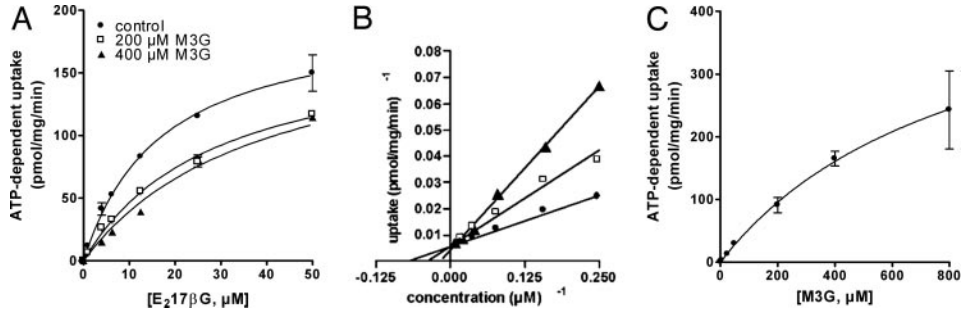

Fig. 1. Transport of M3G by MRP3. (*A*) Concentration-dependent transport of [^{3}H]$E_2$17βG by MRP3 in the presence or absence of M3G. (*B*) Lineweaver–Burk transformations of the data presented. (*C*) Concentration-dependent uptake of [^{3}H]M3G by MRP3. Values are corrected for transport in the absence of ATP. Each data point and error are mean ± SD of experiments in triplicate.

end of the assay, the cells were washed with cold PBS and subsequently collected and stored at −80°C until analysis. Expression levels of MRP3 and UGT2B7 were determined in total cell lysates by immunoblot analysis with monoclonal antibody M_3II9 (1:250) (19) and the human UGT2B7 Western blotting kit (Gentest, Alphen aan de Rijn, The Netherlands), respectively.

Preparation of Membrane Vesicles and Vesicular Transport Assays. ATP-dependent transport of [^{3}H]$E_2$17βG and [^{3}H]M3G into inside-out membrane vesicles prepared from *Spodoptera frugiperda* cells overproducing MRP3 was measured by using the rapid filtration technique, as described (21, 24).

Animals. *Mrp3*$^{(-/-)}$ mice have been generated in our laboratory recently and are described elsewhere (25). The *Mrp3*$^{(-/-)}$ and WT mouse colonies were maintained as a cross of FVB and 129/Ola (50%/50%), because the 129/Ola mice breed poorly. *In vivo* experiments with M6G were done with *Mrp3*$^{(-/-)}$ mice backcrossed (99%) in an FVB genetic background. Other animals used in this study were *Mrp1*$^{(-/-)}$ (26) and *Mrp4*$^{(-/-)}$ mice (27). All animals received food and water ad libitum and were housed in constant temperature rooms with a 12-h light/12-h dark cycle. Mouse handling and experimental procedures were conducted in accordance with institutional guidelines for animal care and use.

Analysis of Morphine Pharmacokinetics in Mice. Age-, gender-, and weight-matched mice were fasted overnight before the onset of each experiment. Mice were injected i.p. with the indicated dose of morphine, M3G, or M6G. For the time-course experiments, three mice of each group (WT and *Mrp3*$^{(-/-)}$) were killed at each time point by heart blood sampling under methoxyflurane anesthesia. Subsequently, liver, brain, and gall bladder bile were collected. Blood was collected in tubes containing heparin, and plasma was obtained after centrifugation for 10 min at 1,300 × *g* at 22°C and stored at −80°C until analysis. M3G concentrations in micromolar in liver tissue were calculated from the amounts detected as nanogram of M3G per milligram of liver tissue by using the molecular weight of M3G (461.5 g/mol) and assuming that 1 g of liver tissue has a volume of 1 ml. To analyze the urinary excretion of morphine and its metabolites, mice were placed in metabolic cages 3 days before morphine injection. One day before morphine injection, chow was removed. The next day, morphine was injected as described above and urine collected during the next 24 h. At the end of the experiment, mice were killed, as mentioned above.

Analysis of Antinociceptive Effects. Hot-plate and tail-immersion tests were performed as described by Matthes *et al.* (28). In short, the latency in the antinociceptive response in the hot-plate test (53°C, cutoff value of 30 s to prevent tissue damage) and tail-immersion test (54°C, cutoff value of 15 s) were determined at the indicated time points after i.p. administration of M6G (10 mg/kg). The following antinociceptive responses were used: hindpaw licking/hindpaw shaking for the hot-plate test and a rapid tail flick for the tail-immersion test. Baseline latencies were determined before the onset of each experiment in triplicate for each individual animal. Experiments were done blind. Data were converted to percentage of maximal possible effect (MPE) by using the following equation: %MPE = (postdrug latency − baseline latency)/(cutoff latency − baseline latency) × 100. Values presented are mean ± SEM.

Tissue Distribution of [^{3}H]Morphine. Mice were injected i.p. with [^{3}H]morphine (15 mg/kg; 1–1.5 μCi per mouse). Thirty minutes or 24 h after injection, mice were killed as described above and tissues collected, weighed, and solubilized by using Solvable, as described by the manufacturer (Packard Biosciences, Groningen, The Netherlands). After solubilization, samples were bleached by using H_2O_2. The level of radioactivity in tissue homogenates was determined by liquid scintillation counting by using Ultima Gold scintillation fluid (Packard Biosciences).

Analysis and Detection of Morphine, M3G, and M6G. Analysis of morphine and its metabolites in cell culture medium, plasma, and urine was done as described by Rook *et al.* (29). Bile was diluted in running buffer and directly injected into the liquid chromatography tandem MS apparatus. Liver and brain tissue were first homogenized in 5 and 3 ml of human plasma, respectively. Subsequently, a sample of 50 μl was drawn of the homogenates and treated like the plasma samples.

Statistical Analysis. Differences between groups were evaluated with Student's *t* test, and the statistical significance of differences is indicated in Figs. 1–5.

Results

Transport of M3G and M6G by MRP3 in Vesicular Uptake Experiments. To study the ability of MRP3 to interact with M3G/M6G, we tested whether these morphine-glucuronides inhibit MRP3-mediated transport of $E_2$17βG, an established MRP3 substrate (23, 24), in vesicular uptake experiments. At a concentration of 430 μM, both compounds inhibited MRP3-mediated transport of 1 μM [^{3}H]$E_2$17βG (Fig. 6, which is published as supporting information on the PNAS web site). Inhibition of MRP3 by M3G was competitive, with a K_i of ≈290 μM (Fig. 1 *A* and *B*). Because M3G is not commercially available in radioactive form, we prepared [^{3}H]M3G from the urine of mice injected with [^{3}H]morphine (see *Materials and Methods*). Fig. 1*C* shows that [^{3}H]M3G is transported by MRP3 at a high rate but with low affinity (K_m in the range of 500–1,000 μM). HPLC analysis (30) was used to verify that the [^{3}H] label taken up by the vesicles was exclusively M3G (data not shown). Additionally, no direct transport of [^{3}H]morphine into inside-out membrane vesicles containing MRP3 was detected (data not shown).

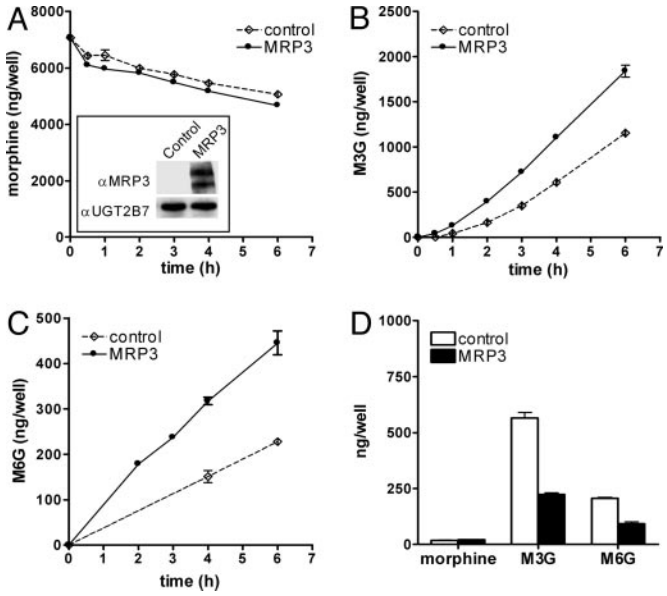

Fig. 2. Cellular efflux of M3G and M6G by HEK293 cells coexpressing UGT2B7 and MRP3. (*A*) Time curve of the amount of morphine in the cell culture medium. (*B* and *C*) Cumulative amounts of M3G (*B*) and M6G (*C*) secreted in the cell culture medium (note that during the first 2–4 h of the experiments, M6G concentrations were below the detection limit of the assay). (*D*) Amounts of morphine, M3G, and M6G in the cell pellet at the end of the experiment. Values shown are mean ± SD of an experiment in triplicate. The data shown are representative of three independent experiments. (*A Inset*) Immunoblot analysis of the cells used; MRP3 is present as a double band, as described (19).

Efflux of M3G and M6G from HEK293 Cells Coexpressing UGT2B7 and MRP3. The construction of HEK293 cells containing the glucuronosyl transferase UGT2B7 in combination with MRP3 allowed us to generate M3G and M6G from morphine intracellularly and follow their efflux over time. Transient transfection of HEK293-UGT2B7 cells with the MRP3 cDNA construct resulted in high levels of MRP3 protein (Fig. 2*A Inset*). Incubation of these cells with morphine (10 μM) resulted in a gradual decrease in the morphine levels in the cell culture medium that was hardly influenced by the presence of MRP3 (Fig. 2*A*). However, MRP3 did increase the efflux of both morphine-glucuronides, as reflected by their earlier appearance and higher overall levels in the cell culture medium (Fig. 2 *B* and *C*). The high rate of endogenous transport of morphine glucuronides in the absence of MRP3 (Fig. 2 *B* and *C*) could be due to the substantial levels of MRP1 present in HEK293 cells, because it was partially inhibited by 10 μM MK571, a compound known to inhibit several MRPs (data not shown). The increased efflux of morphine-glucuronides from MRP3-containing cells was mirrored by decreased intracellular accumulation of these compounds, whereas the intracellular amount of morphine was not altered (Fig. 2*D*). The higher levels of M3G than M6G in the medium and in the cells reflect the preferential formation by UGT2B7 of the 3- over the 6-glucuronide (6). Within the 6-h time frame of these experiments, 25–30% of the morphine was converted to M3G and M6G, and the overall mass balance varied between 95% and 105% (data not shown).

Pharmacokinetics of Morphine in *Mrp3*$^{(-/-)}$ Mice. To assess the contribution of MRP3 to the transport of morphine-glucuronides *in vivo*, we compared morphine disposition in WT and in the *Mrp3*$^{(-/-)}$ mice after the i.p. administration of morphine (15 mg/kg). Mice differ from humans in their morphine metabolism: in humans, morphine is converted into M3G and M6G, whereas mice form only M3G (31). Conversion of morphine to M3G and its export from the liver is a fast process, because plasma concentrations of M3G already exceed those of morphine after 5 min in WT mice (Fig. 3 *A* and *B*; note the difference in scale between *A* and *B*). Plasma morphine levels were similar in *Mrp3*$^{(-/-)}$ and WT mice (Fig. 3*A*). However, a profound difference was found in plasma M3G: it was very high in WT mice and very low in *Mrp3*$^{(-/-)}$ mice. The lower M3G plasma concentrations were specific for *Mrp3*$^{(-/-)}$ mice; knockout mice lacking Mrp1, another sinusoidal transporter, had similar M3G concentrations as WT mice 30 min after morphine injection (Fig. 3*H*). Urinary excretion of M3G in *Mrp3*$^{(-/-)}$ mice was strongly decreased, whereas the total amount of morphine excreted was slightly but significantly increased (Fig. 3*C*). Consistent with impaired cellular efflux of M3G from hepatocytes into the circulation, we found increased hepatic levels of M3G in *Mrp3*$^{(-/-)}$ mice (Fig. 3*D*). M3G concentrations in bile were also increased in the *Mrp3*$^{(-/-)}$ mice, both 30 min and 24 h after morphine administration (Fig. 3 *E* and *F*), showing a shift from sinusoidal to

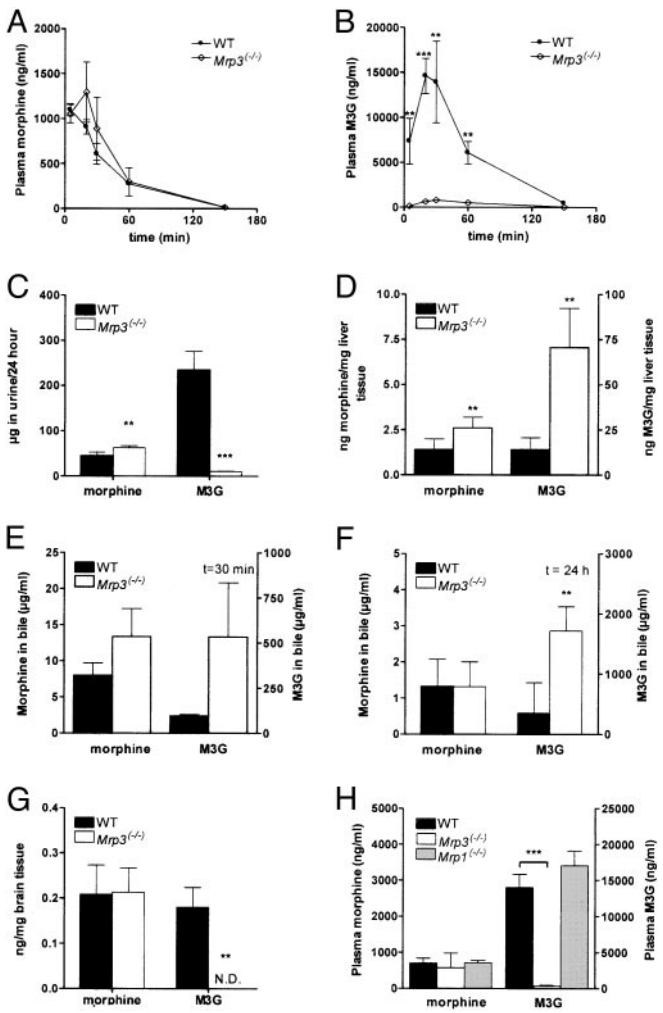

Fig. 3. Pharmacokinetics of morphine in WT and *Mrp3*$^{(-/-)}$ mice. Groups of mice (n = 3 or 4 per time point) received a dose of 15 mg of morphine per kg i.p. Plasma concentrations of morphine (*A*) and M3G (*B*) were determined at the indicated time points. (*C*) Total urinary excretion of morphine and M3G over 24 h. (*D*) Morphine and M3G concentration in liver 30 min after morphine injection. Concentrations of morphine and M3G in bile 30 min (*E*) and 24 h (*F*) after morphine injection. (*G*) Morphine and M3G concentration in brain 30 min after morphine injection. M3G levels in brain of *Mrp3*$^{(-/-)}$ mice were below the detection limit and not detectable (N.D.). (*H*) Plasma concentrations of morphine and M3G in WT, Mrp1$^{(-/-)}$, and Mrp3$^{(-/-)}$ mice, 30 min after morphine injection. Values shown are means ± SD. **, $P < 0.01$; ***, $P < 0.001$ comparing *Mrp3*$^{(-/-)}$ with WT mice.

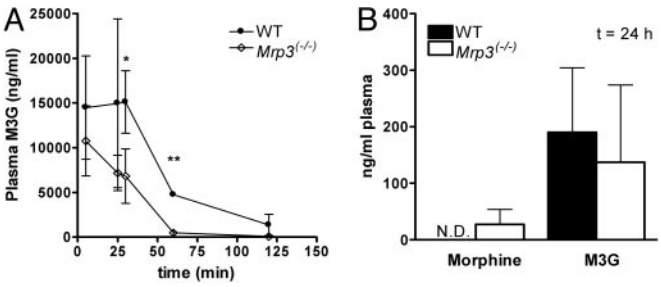

Fig. 4. Pharmacokinetics of M3G in WT and *Mrp3*$^{(-/-)}$ mice. Groups of mice ($n = 3$ per time point) received a dose of 24 mg of M3G per kg i.p. (*A*) Plasma concentration of M3G was determined at the indicated time points after injection. (*B*) Plasma concentrations of morphine and M3G after 24 h. Values shown are means ± SD. *, $P < 0.05$; **, $P < 0.01$, for *Mrp3*$^{(-/-)}$ compared with WT mice; N.D., not detected.

canalicular excretion of M3G in the absence of Mrp3. Brain morphine levels were similar in *Mrp3*$^{(-/-)}$ and WT mice 30 min after morphine administration. However, M3G was below the detection limit of the assay in brain tissue of *Mrp3*$^{(-/-)}$ mice, whereas it was readily detected in WT mice (Fig. 3*G*). The absence of M3G in the brain and the lower levels in the urine of *Mrp3*$^{(-/-)}$ mice are obviously due to the lower plasma levels of M3G in these animals.

To find out whether the decreased excretion of M3G via the urine and the lower M3G level in brain tissue of *Mrp3*$^{(-/-)}$ mice were due only to impaired sinusoidal excretion of newly formed M3G from the liver, we administered M3G (24 mg/kg, equimolar to 15 mg of morphine per kg) i.p. to mice and followed concentrations of M3G in plasma over time (Fig. 4*A*). We also determined morphine/M3G levels in liver and brain and the cumulative 24-h urinary excretion of both compounds (Table 1). Maximum M3G concentrations in WT mice were similar to those found after injection of morphine (compare Figs. 3*B* and 4*A*). Unexpectedly, *Mrp3*$^{(-/-)}$ mice had lower M3G plasma concentrations, a difference reaching statistical significance after 30 and 60 min (Fig. 4*A*). Moreover, 24-h urinary excretion of M3G was also lowered in *Mrp3*$^{(-/-)}$ mice (Table 1), similar to what was found after morphine injection (Fig. 3*C*). The concentration of M3G in liver tissue was increased (Table 1), indicating that the liver actively takes up M3G from the circulation and, in the absence of Mrp3, redirects it into bile. Interestingly, low levels of morphine were detected in the plasma of *Mrp3*$^{(-/-)}$ mice 24 h after the M3G injection but not in WT mice (Fig. 4*B*), indicating that there is increased enterohepatic circulation (EHC) of morphine/M3G in *Mrp3*$^{(-/-)}$ mice. After injection of M3G, differences in plasma M3G levels were accompanied by similar differences in M3G brain tissue concentrations (Table 1), suggesting again that brain M3G concentration largely depends on the level found in plasma.

Tissue Disposition of [^{3}H]Morphine in WT and *Mrp3*$^{(-/-)}$ Mice. The 24-h urinary excretion of morphine and M3G accounts for ≈65% of the administered morphine dose in WT but only 25% in *Mrp3*$^{(-/-)}$ mice (Table 1 and Fig. 3*C*). To determine where the remainder of the morphine in WT and *Mrp3*$^{(-/-)}$ mice was, the tissue distribution of [^{3}H]morphine (15 mg/kg) was analyzed 30 min and 24 h after injection (Table 2). At both time points, the amount of label detected in tissues involved in the urinary excretion pathway (kidney, bladder, and urine) was significantly higher in WT than in *Mrp3*$^{(-/-)}$ mice. The opposite was found in several tissues involved in excretion via the gastrointestinal (GI) tract (liver, bile, small intestine, and intestinal content). These results indicate that loss of Mrp3 results in a shift from urinary excretion to excretion via the GI tract. Consistent with the results of Fig. 3*D*, showing higher M3G concentrations in livers of *Mrp3*$^{(-/-)}$ than of WT mice, the level of radiolabel detected in the livers of *Mrp3*$^{(-/-)}$ mice was substantially higher than in the livers of WT controls, whereas the lower levels of radiolabel detected in *Mrp3*$^{(-/-)}$ brain tissue (Table 2) were in agreement with the absence of M3G in brain tissue of knockout mice (Fig. 3*G*). Because the amount of morphine equivalent detected in urine, liver, and brain by liquid chromatography tandem MS (Fig. 3) corresponded with that detected after injection of [^{3}H]morphine (Table 2), we can rule out that, in the absence of Mrp3, substantial amounts of other metabolites than M3G are formed. Total recovery of label was 62 ± 4% after 30 min and 90 ± 3% after 24 h (Table 2). The incomplete recovery can be explained by the fact that not all tissues were analyzed for label content (e.g., radioactivity in bones and skin was not determined) and by incomplete recovery of urine and feces from the metabolic cages.

M6G Induced Antinociception in WT and *Mrp3*$^{(-/-)}$ Mice. Although M6G is not formed in mice (31, 32), in humans, this compound is formed in the liver and contributes to the pharmacological effect of morphine (6), resulting in an increasing interest in the usage of M6G as a postoperative analgesic (8). M6G is transported by MRP3 (Fig. 2*C*). We reasoned that if M6G has similar pharmacokinetics as M3G in the absence of Mrp3 (Fig. 4 and Table 1), this would also have pharmacological implications for M6G. Consistent with this hypothesis, the absence of Mrp3 resulted in lower M6G plasma levels 60 min after M6G administration (24 mg/kg, equimolar to 15 mg/kg morphine; Fig. 5*A*) and in decreased antinociception of M6G (i.p., 10 mg/kg) in *Mrp3*$^{(-/-)}$ mice, as reflected by a decrease in the area under the time curve in hot-plate and tail-immersion experiments (Fig. 5 *C* and *D*; $P < 0.01$ and $P < 0.05$, respectively). The appearance of M3G after the administration of M6G to WT mice is indicative of the presence of EHC (Fig. 5*B*). The morphine taken up from the gut after EHC of M6G is readily converted into M3G, which is transported into the circulation in WT mice but not in *Mrp3*$^{(-/-)}$ mice. Because also enterocytes glucuronidate morphine (33), it is not known whether the M3G is formed in the gut or in the liver.

Discussion

Not much information is available about the physiological function of MRP3. Its involvement in clinically relevant drug resistance of tumors seems limited (16, 17). Initial attempts to find another

Table 1. Levels of morphine and M3G in urine, liver, and brain after M3G administration

	Morphine		M3G	
Tissue/excretion product	WT	*Mrp3*$^{(-/-)}$	WT	*Mrp3*$^{(-/-)}$
Urinary excretion, μg/24 h	13.8 ± 0.7	22 ± 8.1	236 ± 4	42.0 ± 12.2 ***
Liver, ng/mg of tissue	0.16 ± 0.06	0.24 ± 0.07	51 ± 19	85 ± 13
Brain, ng/mg of tissue	ND	ND	0.91 ± 0.13	0.48 ± 0.34

Levels of morphine and M3G in liver, brain, and urine after the administration of M3G to WT and *Mrp3*$^{(-/-)}$ mice. Levels in liver and brain were determined 30 min after injection of M3G (24 mg/kg, i.p.), whereas, in urine, the amounts excreted during 24 h were determined. Data are expressed as means ± SD. ND, not detected. ***, $P < 0.001$, for *Mrp3*$^{(-/-)}$ compared with WT mice.

Table 2. Levels of radioactivity in tissues and excretion products of *Mrp3*$^{(-/-)}$ and WT mice after [^{3}H]morphine administration

Tissue	WT (30 min)	*Mrp3*$^{(-/-)}$ (30 min)	WT (24 h)	*Mrp3*$^{(-/-)}$ (24 h)
Blood	0.37 ± 0.01	0.09 ± 0.01***	0.05 ± 0.01	0.05 ± 0.004
Lung	0.44 ± 0.03	0.26 ± 0.04**	0.04 ± 0.007	0.04 ± 0.004
Brain	0.09 ± 0.002 (0.05 ± 0.01)	0.06 ± 0.01** (0.03 ± 0.001)	0.06 ± 0.003	0.06 ± 0.007
Liver	5.7 ± 0.5 (4.2 ± 1.8)	15.9 ± 1.2*** (13.5 ± 1.3)	0.49 ± 0.1	1.2 ± 0.2**
Gall bladder	0.31 ± 0.24	3.1 ± 1.4*	1.2 ± 0.4	2.4 ± 0.5**
Kidney	4.6 ± 0.3	1.6 ± 0.1***	0.23 ± 0.05	0.19 ± 0.02
Urine bladder	27.8 ± 3.8	11.6 ± 1.3**	2.0 ± 0.3	0.69 ± 0.9*
Urine	ND	ND	55.9 ± 10.9 (67.6 ± 12.8)	29.5 ± 5.2** (23.8 ± 2.3)
Stomach	1.3 ± 0.3	1.8 ± 0.1	0.13 ± 0.05	0.14 ± 0.02
Stomach cont	0.42 ± 0.12	4.6 ± 2.1*	0.10 ± 0.09	0.12 ± 0.10
Small intestine	14.5 ± 2.3	17.9 ± 5.7	3.5 ± 1.9	8.0 ± 2.7*
Colon + cecum	2.6 ± 0.37	2.4 ± 0.33	2.5 ± 1.1	4.3 ± 0.75*
Intestinal cont	1.2 ± 0.9	3.5 ± 2.7	24.7 ± 6.9	42.1 ± 6.6**
Total gastrointestinal tract†	20.1 ± 1.8	30.2 ± 1.2**	31.0 ± 9.0	54.7 ± 4.6**
Total recovery	60.9 ± 5.9	64.1 ± 2.6	91.1 ± 1.6	88.9 ± 4.1

Tissue distribution and excretion of administered [^{3}H]morphine in *Mrp3*$^{(-/-)}$ and WT mice. Groups of mice (n = 3 or 4 per time point) were injected with a dose of 15 mg/kg [^{3}H]morphine i.p., and, 30 min or 24 h later, distribution of [^{3}H]label in the indicated tissues and excretion products was determined by liquid scintillation counting. Data are expressed as percent of the total dose administered. Values between brackets represent the percentage of the total administered dose of morphine detected as morphine and M3G by liquid chromatography MS and are taken from the data in Fig. 3. ND, not determined. Values shown are means ± SD.

†Cumulative percentage of label detected in stomach, stomach content, small intestine, cecum, colon, and intestinal content. *, $P < 0.05$; **, $P < 0.01$; ***, $P < 0.001$ for *Mrp3*$^{(-/-)}$ compared with WT mice.

function focused on the role of MRP3 in the reabsorption of bile acids in the ileum and in the protection of the liver against the toxic effects of bile acids accumulating intrahepatically when bile flow is impaired (21, 34–36). Experiments with *Mrp3*$^{(-/-)}$ mice failed to confirm such roles for murine Mrp3, however (25). An alternative hypothesis is that MRP3 participates in the detoxification of both endogenous and exogenous compounds (37), and this hypothesis was further explored in this article.

Glucuronidation, catalyzed by specific UGTs, represents a major detoxification pathway of endogenous and exogenous compounds (38). Morphine is a model compound used to study glucuronidation (6), which occurs predominantly in the liver. In humans, morphine glucuronidation is catalyzed by UGT2B7, resulting in the formation of M3G and M6G (6). In mice, a different UGT isoform is involved, and only M3G is formed (31, 32). To prevent the intracellular accumulation of the hydrophilic morphine-glucuronides after their formation, they must be transported by specific carriers out of the hepatocytes.

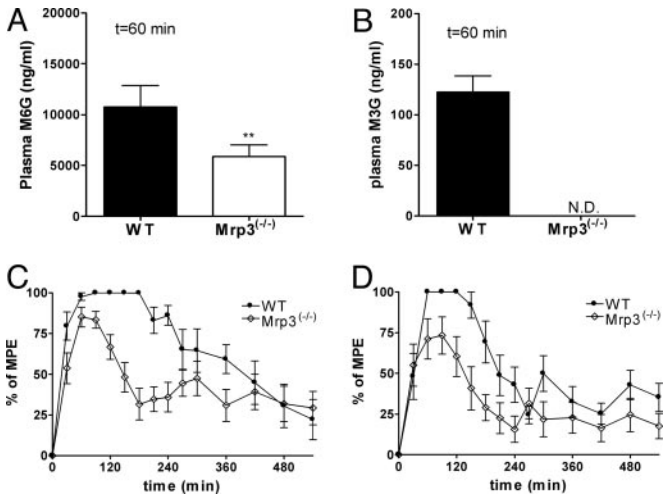

Fig. 5. Pharmacokinetics and pharmacodynamics of M6G in WT and *Mrp3*$^{(-/-)}$. (*A* and *B*) Groups of mice (n = 5 per group) received a dose of 24 mg/kg M6G i.p., and, 60 min later, plasma concentrations of M6G (*A*) and M3G (*B*) were determined. (*C* and *D*) Time curve of the antinociceptive effect of M6G (10 mg/kg, i.p.), as determined by hot-plate (*C*) and tail-immersion (*D*) tests (n = 10–12 per group). The area under the curve differed significantly between *Mrp3*$^{(-/-)}$ and WT mice in hot-plate ($P < 0.01$) and tail-immersion ($P < 0.05$) tests.

Because our in *vitro* experiments (Figs. 1 and 2) indicated that MRP3 transports morphine-glucuronides, we tested the effect of a complete loss of Mrp3 on morphine pharmacokinetics in *Mrp3*$^{(-/-)}$ mice (25). As shown in Fig. 3, the loss of Mrp3 resulted in drastically lowered plasma concentrations (Fig. 3*B*) and decreased urinary excretion (Fig. 3*C*) of M3G. Concomitantly, the levels of M3G in liver (Fig. 3*D*) and bile (Fig. 3 *E* and *F*) increased 5-fold. Even in these extreme conditions, no M6G was detectable, in agreement with previous reports (31, 32). Taken collectively, our results show that Mrp3 is the major, if not the only, transporter able to excrete M3G from hepatocytes into the bloodstream. In agreement with this conclusion, the absence of another hepatic basolateral transporter known to transport glucuronidated conjugates, Mrp1 [which is known to be very low in liver (39)] did not result in altered morphine pharmacokinetics (Fig. 3*H*).

In the *Mrp3*$^{(-/-)}$ mice, the calculated intrahepatic M3G concentration rises to 160 μM (see *Materials and Methods*) 30 min after an i.p. injection of morphine and results in a brisk excretion of M3G into bile (Fig. 3 *D* and *E*). There are several organic anion transporters present in the canalicular membrane of hepatocytes that might transport M3G into bile (40), including the ABC transporters Abcg2/Bcrp1 (41) and Abcc2/Mrp2 (17). Mrp2 could do the job, because we found in experiments analogous to those presented in Figs. 1 and 2 that Mrp2 can transport M3G (unpublished results).

In the absence of Mrp3, mice shift their excretion of morphine from primarily urinary to primarily biliary (fecal). The M3G excreted into bile can be deglucuronidated in the large intestine by resident bacteria, and the morphine can subsequently be taken up by enterocytes (42). The higher amount of M3G that is excreted into bile in *Mrp3*$^{(-/-)}$ mice might therefore lead to increased EHC, and this might explain the presence of morphine in plasma 24 h after administration of M3G to *Mrp3*$^{(-/-)}$ mice but not to WT mice. Enterocytes are also able to glucuronidate morphine (33), suggesting that Mrp3 present in the basolateral membrane of enterocytes (25) mediates M3G transport from the gut. It is remarkable that the

shift from urinary to biliary excretion of M3G also occurs in *Mrp3*$^{(-/-)}$ mice after the i.p. administration of M3G (Fig. 4) and M6G (Fig. 5) rather than morphine itself. This result was unexpected but implies that hepatocytes have an active uptake system for morphine-glucuronides. Plausible candidates for this uptake system are the members of the solute carrier 21A family (SLC21A, OATP) (43). It is unclear why hepatocytes take up a metabolite that is normally targeted for urinary excretion. Possibly, the uptake system has a broad substrate specificity, which is normally counteracted by specific transporters such as Mrp3, which transport some substrates back into the bloodstream for their urinary excretion. Many glucuronidated compounds are preferentially excreted via the urine and not via the bile, presumably to circumvent the exposure of these metabolites to the intestinal flora that may result in their deglucuronidation, reabsorbtion, and even intestinal toxicity, as is the case with irinotecan (44).

Hepatic MRP3 levels vary among species, which might explain some of the species specificity of morphine pharmacokinetics. For instance, EHC is considerable in rats (42) but not in mice (45). This nicely correlates with the low levels of Mrp3 in rat liver (46) and the high Mrp3 levels in mouse liver (25). Obviously, transporters present in the canalicular membrane are unable to outcompete Mrp3 in the sinusoidal membrane in the normal mouse liver but can take over when Mrp3 is absent. Such a balance between alternative excretion routes for organic anions may apply to drug conjugates other than M3G and to endogenous metabolites as well. We have found, for instance, that after bile duct ligation, the *Mrp3*$^{(-/-)}$ mice have a diminished capacity to transport bilirubin glucuronides from the liver into the bloodstream (25).

Will these dramatically altered pharmacokinetics of morphine and its metabolites in *Mrp3*$^{(-/-)}$ mice have pharmacodynamic implications? Morphine-induced analgesia did not differ between *Mrp3*$^{(-/-)}$ and WT mice (not shown), despite the fact that M3G has been reported to antagonize morphine-induced analgesia (7, 47) and the lower levels of M3G found in brain tissue of *Mrp3*$^{(-/-)}$ mice (Fig. 3*G*). This indicates that the antagonizing effect of M3G on morphine-induced analgesia is at best weak in mice. In contrast, the pharmacokinetics and pharmacodynamics of M6G were clearly influenced by Mrp3 (Fig. 5). Because human MRP3 also transports M6G (Fig. 2*C*), we expect an effect of MRP3 on M6G pharmacokinetics and pharmacodynamics in humans as well. Because the human liver converts morphine into M6G as well as M3G, MRP3 is likely to influence the analgesic potency of morphine by increasing the amount of intrahepatically formed M6G that is transported over the basolateral membrane into the circulation. It follows that genetically determined variations in MRP3 in humans or its induction by other compounds (48) could have an effect on morphine disposition. So far, null alleles of MRP3 have not been described, but polymorphisms in the promoter region of human MRP3 were recently shown to correlate with differences in hepatic MRP3 expression (49). It is therefore possible that part of the differences found in the pharmacokinetics of morphine among individual patients (3) could be due to differences in MRP3 expression.

We thank R. Oude Elferink (Academic Medical Center, Amsterdam) for his important contribution to the characterization of the *Mrp3*$^{(-/-)}$ mouse and A. H. Schinkel for his critical comments. We are grateful to A. J. Schrauwers for his excellent biotechnical assistance. Our research was supported by grants from the Dutch Cancer Society (NKI-2001-2473 and NKI-2001-2474) and The Netherlands Organization of Scientific Research (MW PGS 912-02-073) to R. Oude Elferink and P.B.

1. McQuay, H. (1999) *Lancet* **353,** 2229–2232.
2. Inturrisi, C. E. (2002) *Clin. J. Pain* **18,** S3–S13.
3. Klepstad, P., Dale, O., Kaasa, S., Zahlsen, K., Aamo, T., Fayers, P. & Borchgrevink, P. C. (2003) *Acta Anaesthesiol. Scand.* **47,** 725–731.
4. Yeh, S. Y. (1975) *J. Pharmacol. Exp. Ther.* **192,** 201–210.
5. Mitchell, J. M., Paul, B. D., Welch, P. & Cone, E. J. (1991) *J. Anal. Toxicol.* **15,** 49–53.
6. Coffman, B. L., Rios, G. R., King, C. D. & Tephly, T. R. (1997) *Drug Metab. Dispos.* **25,** 1–4.
7. Moran, T. D. & Smith, P. A. (2002) *J. Pharmacol. Exp. Ther.* **302,** 568–576.
8. Lotsch, J. & Geisslinger, G. (2001) *Clin. Pharmacokinet.* **40,** 485–499.
9. Romberg, R., Olofsen, E., Sarton, E., den Hartigh, J., Taschner, P. E. & Dahan, A. (2004) *Anesthesiology* **100,** 120–133.
10. Thompson, S. J., Koszdin, K. & Bernards, C. M. (2000) *Anesthesiology* **92,** 1392–1399.
11. King, M., Su, W., Chang, A., Zuckerman, A. & Pasternak, G. W. (2001) *Nat. Neurosci.* **4,** 268–274.
12. Bourasset, F., Cisternino, S., Temsamani, J. & Scherrmann, J. M. (2003) *J. Neurochem.* **86,** 1564–1567.
13. Schinkel, A. H., Smit, J. J., van Tellingen, O., Beijnen, J. H., Wagenaar, E., van Deemter, L., Mol, C. A., van der Valk, M. A., Robanus-Maandag, E. C., te Riele, H. P., *et al.* (1994) *Cell* **77,** 491–502.
14. Milne, R. W., Jensen, R. H., Larsen, C., Evans, A. M. & Nation, R. L. (1997) *Pharm. Res.* **14,** 1014–1018.
15. O'Brien, J. A., Nation, R. L. & Evans, A. M. (1996) *J. Pharm. Pharmacol.* **48,** 498–504.
16. Kruh, G. D. & Belinsky, M. G. (2003) *Oncogene* **22,** 7537–7552.
17. Borst, P. & Oude Elferink, R. P. (2002) *Annu. Rev. Biochem.* **71,** 537–592.
18. Konig, J., Rost, D., Cui, Y. & Keppler, D. (1999) *Hepatology* **29,** 1156–1163.
19. Scheffer, G. L., Kool, M., de Haas, M., de Vree, J. M., Pijnenborg, A. C., Bosman, D. K., Elferink, R. P., van der Valk, P., Borst, P. & Scheper, R. J. (2002) *Lab. Invest.* **82,** 193–201.
20. Kool, M., van der Linden, M., de Haas, M., Scheffer, G. L., de Vree, J. M., Smith, A. J., Jansen, G., Peters, G. J., Ponne, N., Scheper, R. J., *et al.* (1999) *Proc. Natl. Acad. Sci. USA* **96,** 6914–6919.
21. Zelcer, N., Saeki, T., Bot, I., Kuil, A. & Borst, P. (2003) *Biochem. J.* **369,** 23–30.
22. Hirohashi, T., Suzuki, H. & Sugiyama, Y. (1999) *J. Biol. Chem.* **274,** 15181–15185.
23. Zeng, H., Liu, G., Rea, P. A. & Kruh, G. D. (2000) *Cancer Res.* **60,** 4779–4784.
24. Zelcer, N., Saeki, T., Reid, G., Beijnen, J. H. & Borst, P. (2001) *J. Biol. Chem.* **276,** 46400–46407.
25. Zelcer, N. (2003) PhD. thesis (University of Amsterdam, Amsterdam), pp. 73–94.
26. Wijnholds, J., Scheffer, G. L., van der Valk, M., van der Valk, P., Beijnen, J. H., Scheper, R. J. & Borst, P. (1998) *J. Exp. Med.* **188,** 797–808.
27. Leggas, M., Adachi, M., Scheffer, G. L., Sun, D., Wielinga, P., Du, G., Mercer, K. E., Zhuang, Y., Panetta, J. C., Johnston, B., *et al.* (2004) *Mol. Cell. Biol.* **24,** 7612–7621.
28. Matthes, H. W., Maldonado, R., Simonin, F., Valverde, O., Slowe, S., Kitchen, I., Befort, K., Dierich, A., Le Meur, M., Dolle, P., *et al.* (1996) *Nature* **383,** 819–823.
29. Rook, E. J., Hillebrand, M. J. X., Rosing, H., van Ree, J. M. & Beijnen, J. H. (2004) *J. Chromatogr. B*, in press.
30. Meng, Q. C., Cepeda, M. S., Kramer, T., Zou, H., Matoka, D. J. & Farrar, J. (2000) *J. Chromatogr. B* **742,** 115–123.
31. Kuo, C. K., Hanioka, N., Hoshikawa, Y., Oguri, K. & Yoshimura, H. (1991) *J. Pharmacobiodyn.* **14,** 187–193.
32. Milne, R. W., Nation, R. L. & Somogyi, A. A. (1996) *Drug Metab. Rev.* **28,** 345–472.
33. Fisher, M. B., Vandenbranden, M., Findlay, K., Burchell, B., Thummel, K. E., Hall, S. D. & Wrighton, S. A. (2000) *Pharmacogenetics* **10,** 727–739.
34. Rost, D., Mahner, S., Sugiyama, Y. & Stremmel, W. (2002) *Am. J. Physiol. Gastrointest. Liver Physiol.* **282,** G720–G726.
35. Bohan, A., Chen, W. S., Denson, L. A., Held, M. A. & Boyer, J. L. (2003) *J. Biol. Chem.* **278,** 36688–36698.
36. Donner, M. G. & Keppler, D. (2001) *Hepatology* **34,** 351–359.
37. Ishikawa, T. (1992) *Trends Biochem. Sci.* **17,** 463–468.
38. Tukey, R. H. & Strassburg, C. P. (2000) *Annu. Rev. Pharmacol. Toxicol.* **40,** 581–616.
39. Pei, Q. L., Kobayashi, Y., Tanaka, Y., Taguchi, Y., Higuchi, K., Kaito, M., Ma, N., Semba, R., Kamisako, T. & Adachi, Y. (2002) *Hepatol. Res.* **22,** 58–64.
40. Suzuki, H. & Sugiyama, Y. (2000) *Semin. Liver Dis.* **20,** 251–263.
41. Maliepaard, M., Scheffer, G. L., Faneyte, I. F., van Gastelen, M. A., Pijnenborg, A. C., Schinkel, A. H., van De Vijver, M. J., Scheper, R. J. & Schellens, J. H. (2001) *Cancer Res.* **61,** 3458–3464.
42. Horton, T. L. & Pollack, G. M. (1991) *J. Pharmacol. Sci.* **80,** 1147–1152.
43. Hagenbuch, B. & Meier, P. J. (2003) *Biochim. Biophys. Acta* **1609,** 1–18.
44. Kuhn, J. G. (1998) *Oncology* **12,** 39–42.
45. Handal, M., Grung, M., Skurtveit, S., Ripel, A. & Morland, J. (2002) *Pharmacol. Biochem. Behav.* **73,** 883–892.
46. Hirohashi, T., Suzuki, H., Ito, K., Ogawa, K., Kume, K., Shimizu, T. & Sugiyama, Y. (1998) *Mol. Pharmacol.* **53,** 1068–1075.
47. Smith, M. T., Watt, J. A. & Cramond, T. (1990) *Life Sci.* **47,** 579–585.
48. Cherrington, N. J., Slitt, A. L., Maher, J. M., Zhang, X. X., Zhang, J., Huang, W., Wan, Y. J., Moore, D. D. & Klaassen, C. D. (2003) *Drug Metab. Dispos.* **31,** 1315–1319.
49. Lang, T., Hitzl, M., Burk, O., Mornhinweg, E., Keil, A., Kerb, R., Klein, K., Zanger, U. M., Eichelbaum, M. & Fromm, M. F. (2004) *Pharmacogenetics* **14,** 155–164.